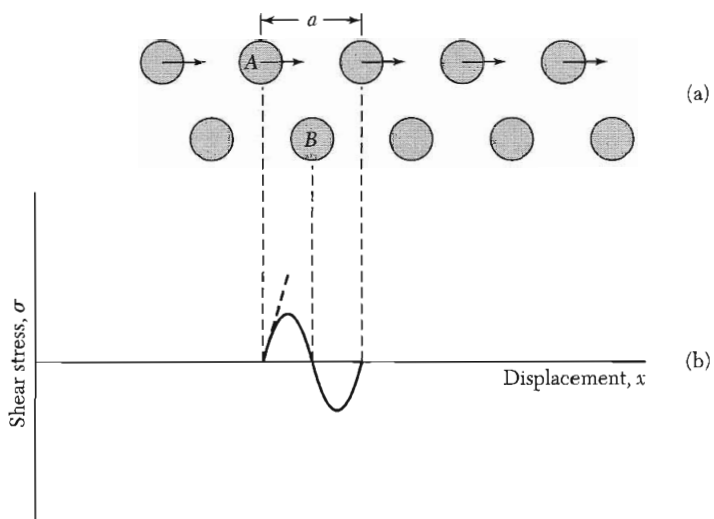


# 21

## *Dislocations*

---

<b>SHEAR STRENGTH OF SINGLE CRYSTALS</b>	<b>599</b>
<i>Slip</i>	<b>600</b>
<b>DISLOCATIONS</b>	<b>601</b>
Burgers vectors	<b>604</b>
Stress fields of dislocations	<b>605</b>
Low-angle grain boundaries	<b>607</b>
Dislocation densities	<b>610</b>
Dislocation multiplication and slip	<b>611</b>
<b>STRENGTH OF ALLOYS</b>	<b>613</b>
<b>DISLOCATIONS AND CRYSTAL GROWTH</b>	<b>615</b>
Whiskers	<b>616</b>
<b>HARDNESS OF MATERIALS</b>	<b>617</b>
<b>PROBLEMS</b>	<b>618</b>
1. Lines of closest packing	<b>618</b>
2. Dislocation pairs	<b>618</b>
3. Force on dislocation	<b>618</b>



**Figure 1** (a) Relative shear of two planes of atoms (shown in section) in a uniformly strained crystal; (b) shear stress as a function of the relative displacement of the planes from their equilibrium position. The heavy broken line drawn at the initial slope defines the shear modulus  $G$ .

## CHAPTER 21: DISLOCATIONS

This chapter is concerned with the interpretation of the plastic mechanical properties of crystalline solids in terms of the theory of dislocations. Plastic properties are irreversible deformations; elastic properties are reversible. The ease with which pure single crystals deform plastically is striking. This intrinsic weakness of crystals is exhibited in various ways. Pure silver chloride melts at 455°C, yet at room temperature it has a cheeselike consistency and can be rolled into sheets. Pure aluminum crystals are elastic (follow Hooke's law) only to a strain of about  $10^{-5}$ , after which they deform plastically.

Theoretical estimates of the strain at the elastic limit of perfect crystals may give values  $10^3$  or  $10^4$  higher than the lowest observed values, although a factor  $10^2$  is more usual. There are few exceptions to the rule that pure crystals are plastic and are not strong: crystals of germanium and silicon are not plastic at room temperature and fail or yield only by fracture. Glass at room temperature fails only by fracture, but it is not crystalline. The fracture of glass is caused by stress concentration at minute cracks.

### SHEAR STRENGTH OF SINGLE CRYSTALS

Frenkel gave a simple method of estimating the theoretical shear strength of a perfect crystal. We consider in Fig. 1 the force needed to make a shear displacement of two planes of atoms past each other. For small elastic strains, the stress  $\sigma$  is related to the displacement  $x$  by

$$\sigma = Gx/d \quad (1)$$

Here  $d$  is the interplanar spacing, and  $G$  denotes the appropriate shear modulus. When the displacement is large and has proceeded to the point that atom  $A$  is directly over atom  $B$  in the figure, the two planes of atoms are in a configuration of unstable equilibrium and the stress is zero. As a first approximation we represent the stress-displacement relation by

$$\sigma = (Ga/2\pi d) \sin(2\pi x/a) \quad (2)$$

where  $a$  is the interatomic spacing in the direction of shear. This relation is constructed to reduce to (1) for small values of  $x/a$ . The critical shear stress  $\sigma_c$  at which the lattice becomes unstable is given by the maximum value of  $\sigma$ , or

$$\sigma_c = Ga/2\pi d \quad (3)$$

If  $a \approx d$ , then  $\sigma_c \approx G/2\pi$ : the ideal critical shear stress is of the order of  $\frac{1}{6}$  of the shear modulus.

**Table 1 Comparison of shear modulus  $G$  and observed elastic limit  $\sigma_c$ <sup>a</sup>**

	Shear modulus $G$ , in dyn/cm <sup>2</sup>	Elastic limit $\sigma_c$ , in dyn/cm <sup>2</sup>	$G/\sigma_c$
Sn, single crystal	$1.9 \times 10^{11}$	$1.3 \times 10^7$	15,000
Ag, single crystal	$2.8 \times 10^{11}$	$6 \times 10^6$	45,000
Al, single crystal	$2.5 \times 10^{11}$	$4 \times 10^6$	60,000
Al, pure, polycrystal	$2.5 \times 10^{11}$	$2.6 \times 10^8$	900
Al, commercial drawn	$\sim 2.5 \times 10^{11}$	$9.9 \times 10^8$	250
Duralumin	$\sim 2.5 \times 10^{11}$	$3.6 \times 10^9$	70
Fe, soft, polycrystal	$7.7 \times 10^{11}$	$1.5 \times 10^9$	500
Heat-treated carbon steel	$\sim 8 \times 10^{11}$	$6.5 \times 10^9$	120
Nickel-chrome steel	$\sim 8 \times 10^{11}$	$1.2 \times 10^{10}$	65

<sup>a</sup>After Mott.

The observations in Table 1 show the experimental values of the elastic limit are much smaller than (3) would suggest. The theoretical estimate may be improved by consideration of the actual form of the intermolecular forces and by consideration of other configurations of mechanical stability available to the lattice as it is sheared. Mackenzie has shown that these two effects may reduce the theoretical ideal shear strength to about  $G/30$ , corresponding to a critical shear strain angle of about 2 degrees. The observed low values of the shear strength can be explained only by the presence of imperfections that can act as sources of mechanical weakness in real crystals. The movement of crystal imperfections called dislocations is responsible for slip at very low applied stresses.

### Slip

Plastic deformation in crystals occurs by slip, an example of which is shown in Fig. 2. In slip, one part of the crystal slides as a unit across an adjacent part. The surface on which slip takes place is known as the slip plane. The direction of motion is known as the slip direction. The great importance of lattice properties for plastic strain is indicated by the highly anisotropic nature of slip. Displacement takes place along crystallographic planes with a set of small Miller indices, such as the {111} planes in fcc metals and the {110}, {112}, and {123} planes in bcc metals.

The slip direction is in the line of closest atomic packing,  $\langle 110 \rangle$  in fcc metals and  $\langle 111 \rangle$  in bcc metals (Problem 1). To maintain the crystal structure after slip, the displacement or slip vector must equal a lattice translation vector. The shortest lattice translation vector expressed in terms of the lattice constant  $a$  in a fcc structure is of the form  $(a/2)(\hat{x} + \hat{y})$ ; in a bcc structure it is  $(a/2)(\hat{x} + \hat{y} + \hat{z})$ . But in fcc crystals one also observes partial displacements which upset the regular sequence  $ABCABC \dots$  of closest-packed planes, to

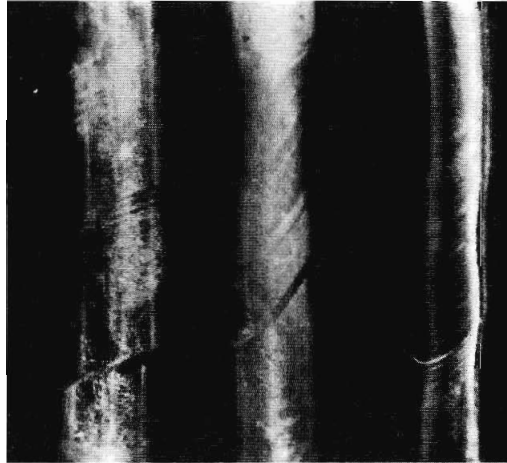


**Figure 2** Translational slip in zinc single crystals. (E. R. Parker.)

produce a **stacking fault** such as  $ABCABABC$ . . . . The result is then a mixture of fcc and hcp stacking.

Deformation by slip is inhomogeneous: large shear displacements occur on a few widely separated slip planes, while parts of the crystal lying between slip planes remain essentially undeformed. A property of slip is the Schmid law of the critical shear stress: slip takes place along a given slip plane and direction when the corresponding *component* of shear stress reaches the critical value.

Slip is one mode of plastic deformation. Another mode, **twinning**, is observed particularly in hcp and bcc structures. During slip a considerable displacement occurs on a few widely separated slip planes. During twinning, a partial displacement occurs successively on each of many neighboring crystallographic planes. After twinning, the deformed part of the crystal is a mirror image of the undeformed part. Although both slip and twinning are caused by the motion of dislocations, we shall be concerned primarily with slip.

## DISLOCATIONS

The low observed values of the critical shear stress are explained in terms of the motion through the lattice of a line imperfection known as a dislocation. The idea that slip propagates by the motion of dislocations was published in 1934 independently by Taylor, Orowan, and Polanyi; the concept of dislocations was introduced somewhat earlier by Prandtl and Dehlinger. There are several basic types of dislocations. We first describe an **edge dislocation**. Figure 3 shows a simple cubic crystal in which slip of one atom distance has occurred over the left half of the slip plane but not over the right half. The boundary between the slipped and unslipped regions is called the dislocation. Its position is marked by the termination of an extra vertical half-plane of atoms crowded into

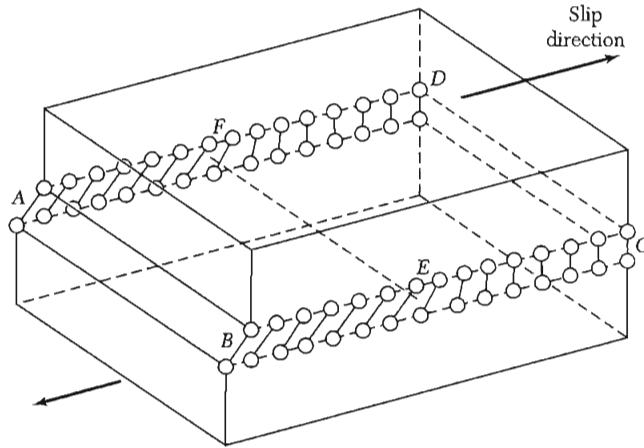


**Figure 3** An edge dislocation  $EF$  in the glide plane  $ABCD$ . The figure shows the slipped region  $ABEF$  in which the atoms have been displaced by more than half a lattice constant and the unslipped region  $FECD$  with displacement less than half a lattice constant.

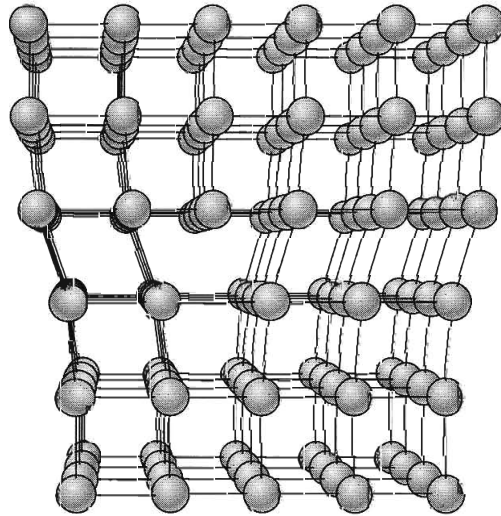


**Figure 4** Structure of an edge dislocation. The deformation may be thought of as caused by inserting an extra plane of atoms on the upper half of the  $y$  axis. Atoms in the upper half-crystal are compressed by the insertion; those in the lower half are extended.

the upper half of the crystal as shown in Fig. 4. Near the dislocation the crystal is highly strained. The simple edge dislocation extends indefinitely in the slip plane in a direction normal to the slip direction. In Fig. 5 we show a photograph of a dislocation in a two-dimensional soap bubble raft obtained by the method of Bragg and Nye.

The mechanism responsible for the mobility of a dislocation is shown in Fig. 6. The motion of an edge dislocation through a crystal is analogous to the passage of a ruck or wrinkle across a rug; the ruck moves more easily than the whole rug. If atoms on one side of the slip plane are moved with respect to

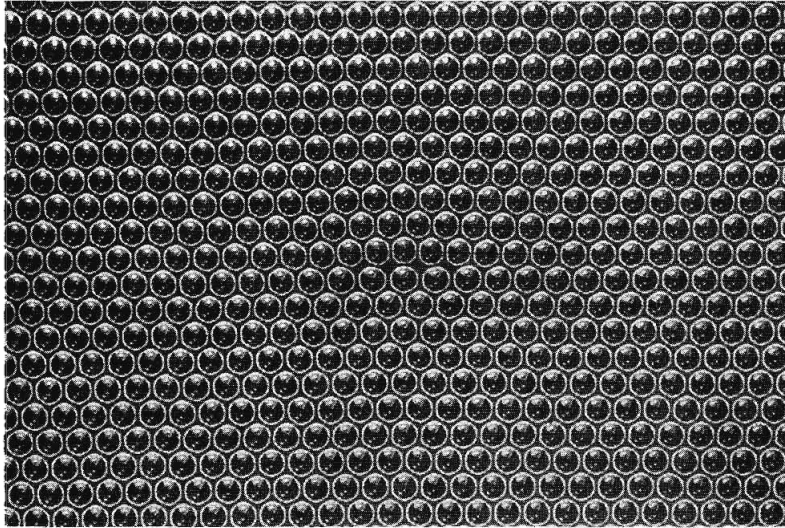


**Figure 5** A dislocation in a two-dimensional bubble raft. The dislocation is most easily seen by turning the page by  $30^\circ$  in its plane and sighting at a low angle. (W. M. Lomer, after Bragg and Nye.)

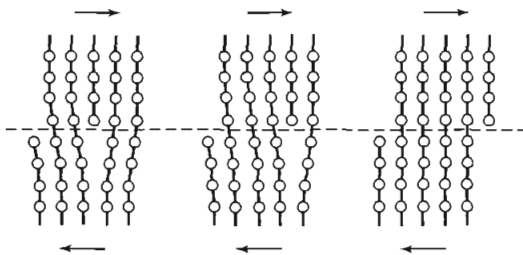


**Figure 6** Motion of a dislocation under a shear tending to move the upper surface of the specimen to the right. (D. Hull.)

those on the other side, atoms at the slip plane will experience repulsive forces from some neighbors and attractive forces from others across the slip plane. These forces cancel to a first approximation. The external stress required to move a dislocation has been calculated and is quite small, below  $10^5$  dyn/cm<sup>2</sup> when the bonding forces in the crystal are not highly directional. Thus dislocations may make a crystal very plastic. Passage of a dislocation through a crystal is equivalent to a slip displacement of one part of the crystal.

The second simple type of dislocation is the **screw dislocation**, sketched in Figs. 7 and 8. A screw dislocation marks the boundary between slipped and unslipped parts of the crystal. The boundary *parallels* the slip direction, instead of lying perpendicular to it as for the edge dislocation. The screw dislocation may be thought of as produced by cutting the crystal partway through with a knife and shearing it parallel to the edge of the cut by one atom spacing. A screw dislocation transforms successive atom planes into the surface of a helix; this accounts for the name of the dislocation.

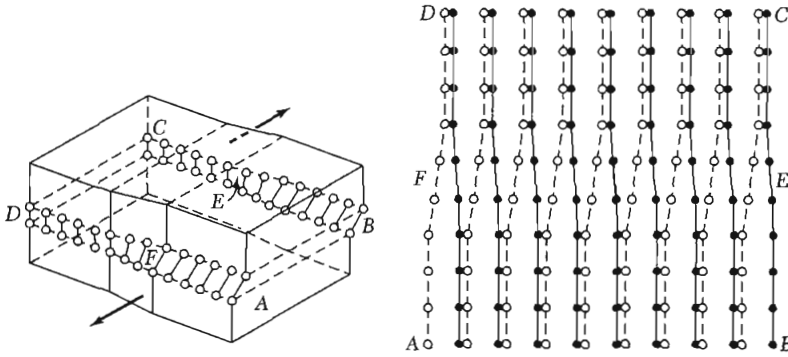


**Figure 7** A screw dislocation. A part  $ABEF$  of the slip plane has slipped in the direction parallel to the dislocation line  $EF$ . A screw dislocation may be visualized as a helical arrangement of lattice planes, such that we change planes on going completely around the dislocation line. (After Cottrell.)

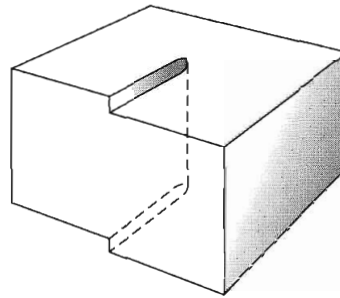


**Figure 8** Another view of a screw dislocation. The broken vertical line that marks the dislocation is surrounded by strained material.

### Burgers Vectors

Other dislocation forms may be constructed from segments of edge and screw dislocations. Burgers has shown that the most general form of a linear dislocation pattern in a crystal can be described as shown in Fig. 9. We consider any closed curve within a crystal, or an open curve terminating on the surface at both ends: (a) Make a cut along any simple surface bounded by the line. (b) Displace the material on one side of this surface by a vector  $\mathbf{b}$  relative to the other side; here  $\mathbf{b}$  is called the **Burgers vector**. (c) In regions where  $\mathbf{b}$  is not parallel to the cut surface, this relative displacement will either produce a gap or cause the two halves to overlap. In these cases we imagine that we either add material to fill the gap or subtract material to prevent overlap. (d) Rejoin the material on both sides. We leave the strain displacement intact at the time of rewelding, but afterwards we allow the medium to come to internal equilibrium. The resulting strain pattern is that of the dislocation characterized jointly by the boundary curve and the Burgers vector. The Burgers vector must be equal to a lattice vector in order that the rewelding process will maintain the crystallinity of the material. The Burgers vector of a screw dislocation (Figs. 7 and 8) is parallel to the dislocation line; that of an edge dislocation (Figs. 3 and 4) is perpendicular to the dislocation line and lies in the slip plane.

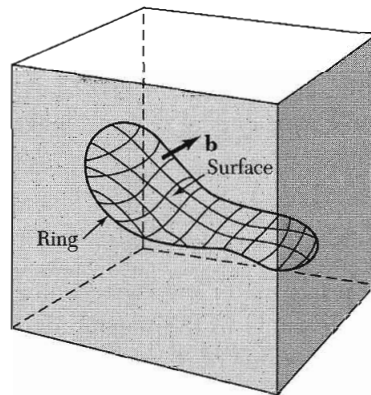


**Figure 9** General method of forming a dislocation ring in a medium. The medium is represented by the rectangular block. The ring is represented by the closed curve in the interior in the block. A cut is made along the surface bounded by the curve and indicated by the contoured area. The material on one side of the cut is displaced relative to that on the other by vector distance  $\mathbf{b}$ , which may be oriented arbitrarily relative to the surface. Forces will be required to effect the displacement. The medium is filled in or cut away so as to be continuous after the displacement. It is then joined in the displaced state and the applied forces are relaxed. Here  $\mathbf{b}$  is the Burgers vector of the dislocation. (After Seitz.)

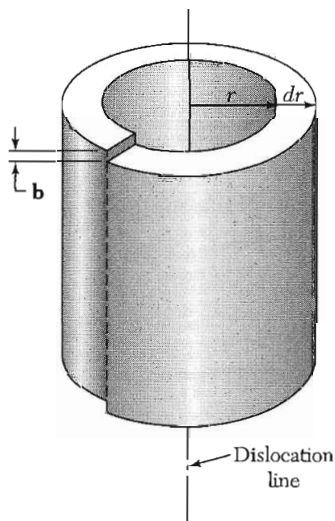


**Figure 10** Shell of elastically distorted crystal surrounding screw dislocation with Burgers vector  $\mathbf{b}$ ; see also Fig. 16.

### ***Stress Fields of Dislocations***

The stress field of a screw dislocation is particularly simple. Figure 10 shows a shell of material surrounding an axial screw dislocation. The shell of circumference  $2\pi r$  has been sheared by an amount  $b$  to give a shear strain  $e = b/2\pi r$ . The corresponding shear stress in an elastic continuum is

$$\sigma = Ge = Gb/2\pi r \quad (4)$$

This expression does not hold in the region immediately around the dislocation line, as the strains here are too large for continuum or linear elasticity theory to apply. The elastic energy of the shell is  $dE_s = \frac{1}{2}Ge^2 dV = (Gb^2/4\pi) dr/r$  per unit length. The total elastic energy per unit length of a screw dislocation is found on integration to be

$$E_s = \frac{Gb^2}{4\pi} \ln \frac{R}{r_0}, \quad (5)$$

where  $R$  and  $r_0$  are appropriate upper and lower limits for the variable  $r$ . A reasonable value of  $r_0$  is comparable to the magnitude  $b$  of the Burgers vector or to the lattice constant; the value of  $R$  cannot exceed the dimensions of the crystal. The value of the ratio  $R/r_0$  is not very important because it enters in a logarithm term.

We now show the form of the energy of an edge dislocation. Let  $\sigma_{rr}$  and  $\sigma_{\theta\theta}$  denote the tensile stresses in the radial and circumferential directions, and let  $\sigma_{r\theta}$  denote the shear stress. In an isotropic elastic continuum,  $\sigma_{rr}$  and  $\sigma_{\theta\theta}$  are proportional to  $(\sin \theta)/r$ ; we need a function that falls off as  $1/r$  and that changes sign when  $y$  is replaced by  $-y$ . The shear stress  $\sigma_{r\theta}$  is proportional to  $(\cos \theta)/r$ ; considering the plane  $y = 0$ , we see from Fig. 4 that the shear stress is an odd function of  $x$ . The constants of proportionality in the stress are proportional to the shear modulus  $G$  and to the Burgers vector  $b$  of the displacement. The final result is

$$\sigma_{rr} = \sigma_{\theta\theta} = -\frac{Gb}{2\pi(1-\nu)} \frac{\sin \theta}{r}, \quad \sigma_{r\theta} = \frac{Gb}{2\pi(1-\nu)} \frac{\cos \theta}{r}, \quad (6)$$

where the Poisson ratio  $\nu \approx 0.3$  for most crystals. The strain energy of a unit length of edge dislocation is

$$E_e = \frac{Gb^2}{4\pi(1-\nu)} \ln \frac{R}{r_0}. \quad (7)$$

We want an expression for the shear stress component  $\sigma_{xy}$  on planes parallel to the slip plane in Fig. 4. From the stress components  $\sigma_{rr}$ ,  $\sigma_{\theta\theta}$ , and  $\sigma_{r\theta}$  evaluated on the plane a distance  $y$  above the slip plane, we find

$$\sigma_{xy} = \frac{Gb}{2\pi(1-\nu)} \cdot \frac{x(x^2 - y^2)}{(x^2 + y^2)^2}. \quad (8)$$

It is shown in Problem 3 that the force caused by a resolved uniform shear stress  $\sigma$  is  $F = b\sigma$  per unit length of dislocation. The force that an edge dislocation at the origin exerts upon a similar one at the location  $(y, \theta)$  is

$$F = b\sigma_{xy} = \frac{Gb^2}{2\pi(1-\nu)} \frac{\sin 4\theta}{4y} \quad (9)$$

per unit length. Here  $F$  is the component of force in the slip direction.

### Low-angle Grain Boundaries

Burgers suggested that low-angle boundaries between adjoining crystal-lites or crystal grains consist of arrays of dislocations. A simple example of the Burgers model of a grain boundary is shown in Fig. 11. The boundary occupies a (010) plane in a simple cubic lattice and divides two parts of the crystal that have a [001] axis in common. Such a boundary is called a pure tilt boundary: the misorientation can be described by a small rotation  $\theta$  about the common [001] axis of one part of the crystal relative to the other. The tilt boundary is represented as an array of edge dislocations of spacing  $D = b/\theta$ , where  $b$  is the Burgers vector of the dislocations. Experiments have substantiated this model. Figure 12 shows the distribution of dislocations along small-angle grain boundaries, as observed with an electron microscope. Further, Read and Shockley derived a theory of the interfacial energy as a function of the angle of tilt, with results in excellent agreement with measurements.

Direct verification of the Burgers model is provided by the quantitative x-ray and optical studies of low-angle boundaries in germanium crystals by Vogel

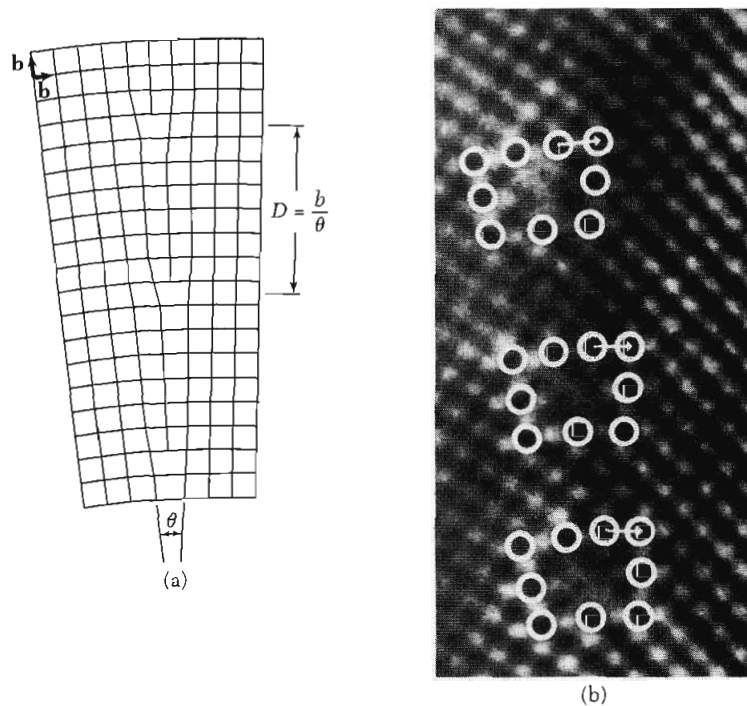


**Figure 11** (a) Low-angle grain boundary, after Burgers. (b) Electron micrograph of a low-angle grain boundary in molybdenum. The three dislocations in the image each have the same Burgers vector as in the drawing in Fig. 11a. The white circles mark the positions of atomic columns normal to the plane of the paper. Each array of circles defines the position of a dislocation, with four circles on the top of each array and three circles below. Closure failure is indicated by the arrows which define the Burgers vectors. (Courtesy of R. Gronsky.)

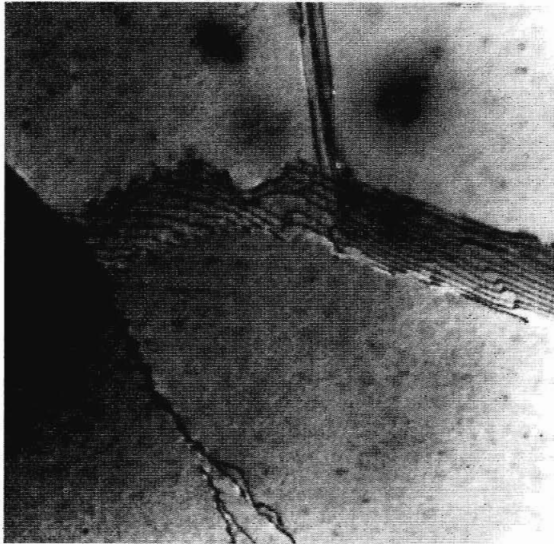


**Figure 12** Electron micrograph of dislocation structures in low-angle grain boundaries in an Al-7 percent Mg solid solution. Notice the lines of small dots on the right. Mag.  $\times 17,000$ . (R. Goodrich and G. Thomas.)

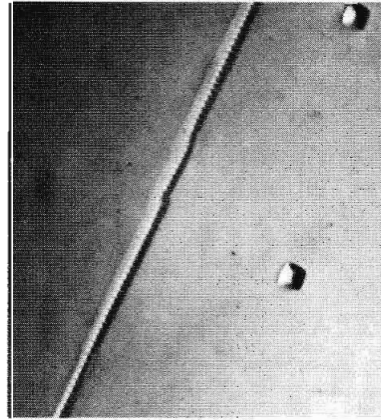


**Figure 13** Dislocation etch pits in low-angle boundary on (100) face of germanium; the angle of the boundary is  $27.5^\circ$ . The boundary lies in a (011) plane; the line of the dislocations is [100]. The Burgers vector is the shortest lattice translation vector, or  $|b| = a/\sqrt{2} = 4.0 \text{ \AA}$ . (F. L. Vogel, Jr.)

and co-workers. By counting etch pits along the intersection of a low-angle grain boundary with an etched germanium surface (Fig. 13), they determined the dislocation spacing  $D$ . They assumed that each etch pit marked the end of a dislocation. The angle of tilt calculated from the relation  $\theta = b/D$  agrees well with the angle measured directly by means of x-rays.

The interpretation of low-angle boundaries as arrays of dislocations is further supported by the fact that pure tilt boundaries move normal to themselves on application of a suitable stress. The motion has been demonstrated in

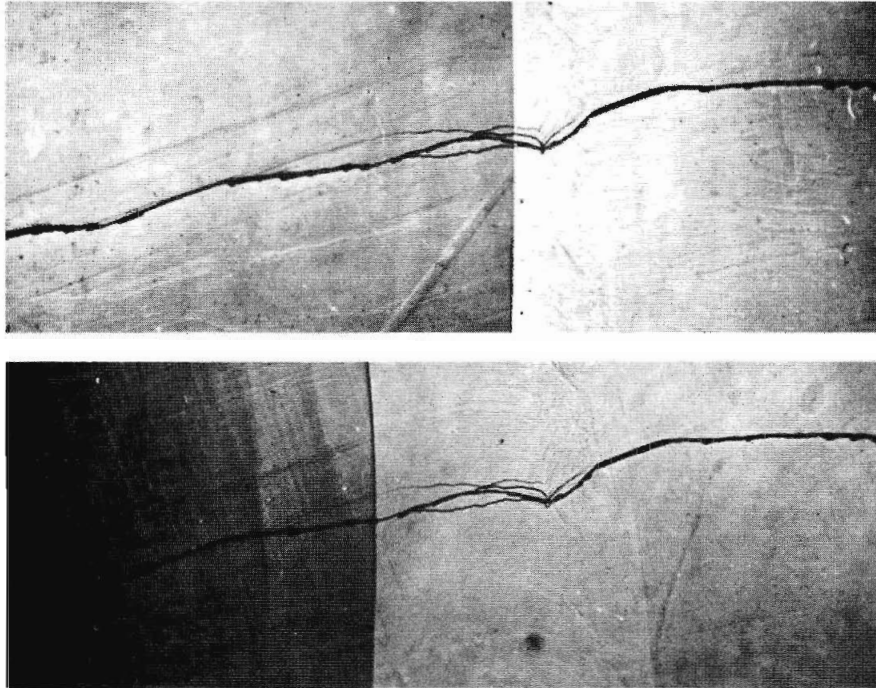


**Figure 14** Motion of a low-angle grain boundary under stress. The boundary is the straight vertical line, and it is photographed under vertical illumination, thereby making evident the  $2^\circ$  angular change in the cleavage surface of the zinc crystal at the boundary. The irregular horizontal line is a small step in the cleavage surface which serves as a reference mark. The crystal is clamped at the left; at the right it is subject to a force normal to the plane of the page. *Top*, original position of boundary; *bottom*, moved back 0.4 mm. (J. Washburn and E. R. Parker.)

a beautiful experiment, Fig. 14. The specimen is a bicrystal of zinc containing a  $2^\circ$  tilt boundary with dislocations about 30 atomic planes apart. One side of the crystal was clamped, and a force was applied at a point on the opposite side of the boundary. Motion of the boundary took place by cooperative motion of the dislocations in the array, each dislocation moving an equal distance in its own slip plane. The motion was produced by stresses of the order of magnitude of the yield stress for zinc crystals, strong evidence that ordinary deformation results from the motion of dislocations.

Grain boundaries and dislocations offer relatively little resistance to diffusion of atoms in comparison with diffusion in perfect crystals. A dislocation is an open passage for diffusion. Diffusion is greater in plastically deformed material than in annealed crystals. Diffusion along grain boundaries controls the rates of some precipitation reactions in solids: the precipitation of tin from lead-tin solutions at room temperature proceeds about  $10^8$  times faster than expected from diffusion in an ideal lattice.

### Dislocation Densities

The density of dislocations is the number of dislocation lines that intersect a unit area in the crystal. The density ranges from well below  $10^2$  dislocations/cm<sup>2</sup> in the best germanium and silicon crystals to  $10^{11}$  or  $10^{12}$  dislocations/cm<sup>2</sup> in heavily deformed metal crystals. The methods available for estimating dislocation densities are compared in Table 2. The actual dislocation configurations in cast or annealed (slowly cooled) crystals correspond either to a group of low-angle grain boundaries or to a three-dimensional network of dislocations arranged in cells, as shown in Fig. 15.

Lattice vacancies that precipitate along an existing edge dislocation will eat away a portion of the extra half-plane of atoms and cause the dislocation to climb, which means to move at right angles to the slip direction. If no dislocations are

**Table 2** Methods for estimating dislocation densities<sup>a</sup>

Technique	Specimen thickness	Width of image	Maximum practical density, per cm <sup>2</sup>
Electron microscopy	>1000 Å	~100 Å	$10^{11}$ – $10^{12}$
X-ray transmission	0.1–1.0 mm	5 μm	$10^4$ – $10^5$
X-ray reflection	<2 μm (min.) – 50 μm (max.)	2 μm	$10^6$ – $10^7$
Decoration	~10 μm (depth of focus)	0.5 μm	$2 \times 10^7$
Etch pits	no limit	0.5 μm <sup>b</sup>	$4 \times 10^8$

<sup>a</sup>W. G. Johnston.

<sup>b</sup>Limit of resolution of etch pits.

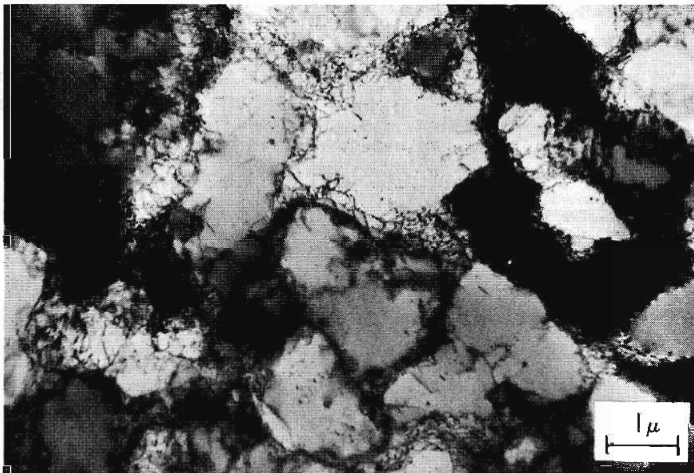


**Figure 15** Cell structure of three-dimensional tangles of dislocations in deformed aluminum. (P. R. Swann.)

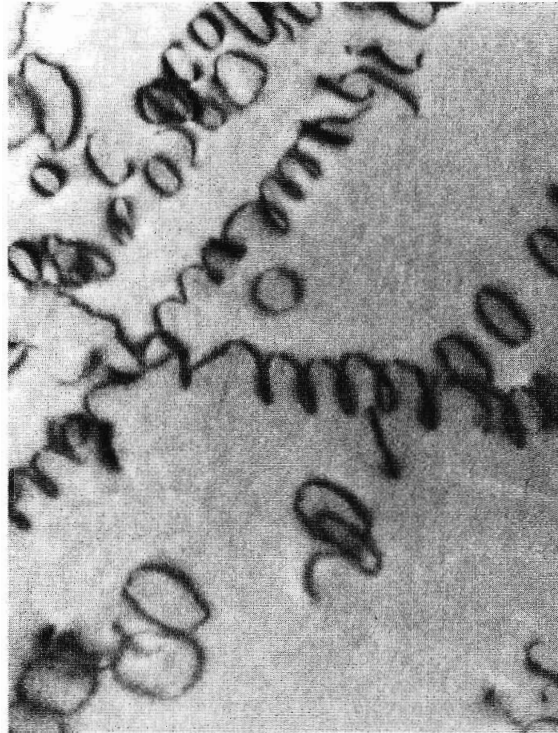


**Figure 16** Electron micrograph of dislocation loops formed by aggregation and collapse of vacancies in Al-5 percent Mg quenched from 550°C. The helical dislocations are formed by vacancy condensation on a screw dislocation. Mag.  $\times 43,000$ . (A. Eikum and G. Thomas.)

present, the crystal will become supersaturated with lattice vacancies; their precipitation in cylindrical vacancy plates may be followed by collapse of the plates and formation of dislocation rings that grow with further vacancy precipitation, as in Fig. 16.

### ***Dislocation Multiplication and Slip***

Plastic deformation causes a very great increase in dislocation density, typically from  $10^8$  to about  $10^{11}$  dislocations/cm<sup>2</sup> during deformation. If a dislocation moves completely across its slip plane, an offset of one atom spacing is produced, but offsets up to 100 to 1000 atom spacings are observed. This means that dislocations multiply during deformation.

Consider a closed circular dislocation loop of radius  $r$  surrounding a slipped area having the radius of the loop. Such a loop will be partly edge, partly screw, and mostly of intermediate character. The strain energy of the loop increases as its circumference, so that the loop will tend to shrink in size. However, the loop will tend to expand if a shear stress is acting that favors slip.

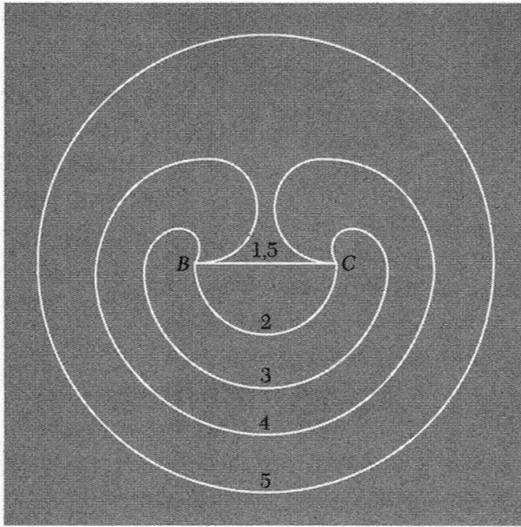


**Figure 17** Frank-Read mechanism for multiplication of dislocations, showing successive stages in the generation of a dislocation loop by the segment *BC* of a dislocation line. The process can be repeated indefinitely.

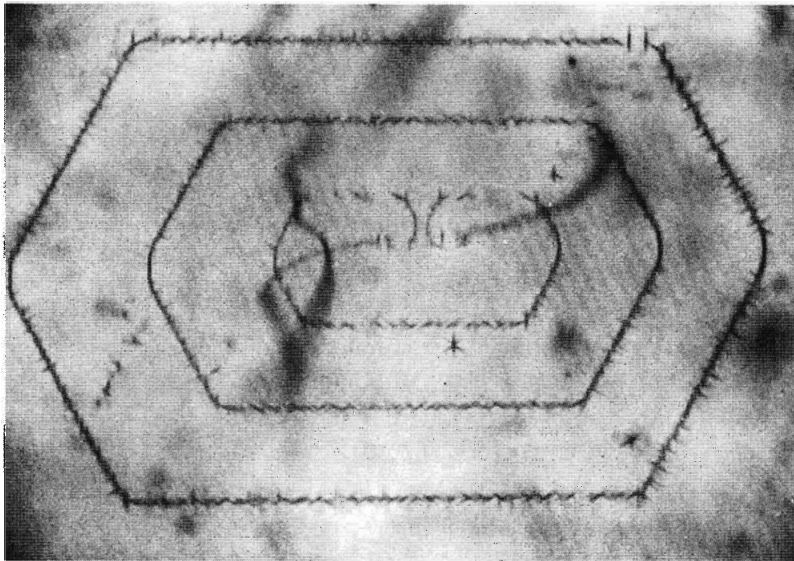


**Figure 18** A Frank-Read dislocation source in silicon, decorated with copper precipitates and viewed with infrared illumination. Two complete dislocation loops are visible, and the third, innermost loop is near completion. (After W. C. Dash.)

A common feature of all dislocation sources is the bowing of dislocations. A dislocation segment pinned at each end is called a **Frank-Read source**, and it can lead (Fig. 17) to the generation of a large number of concentric dislocations on a single slip plane (Fig. 18). Related types of dislocation multiplication mechanisms account for slip and for the increased density of dislocations during plastic deformation. Double cross-slip is the most common source.

### STRENGTH OF ALLOYS

Pure crystals are very plastic and yield at very low stresses. There appear to be four important ways of increasing the yield strength of an alloy so that it will withstand shear stresses as high as  $10^{-2} G$ . They are mechanical blocking of dislocation motion, pinning of dislocations by solute atoms, impeding dislocation motion by short-range order, and increasing the dislocation density so that tangling of dislocations results. All four strengthening mechanisms depend for their success upon impeding dislocation motion. A fifth mechanism, that of removing all dislocations from the crystal, may operate for certain fine hairlike crystals (whiskers) that are discussed in the section on crystal growth.

Mechanical blocking of dislocation motion can be produced most directly by introducing tiny particles of a second phase into a crystal lattice. This process is followed in the hardening of steel, where particles of iron carbide are precipitated into iron, and in hardening aluminum, where particles of  $Al_2Cu$  are precipitated. The pinning of a dislocation by particles is shown in Fig. 19.

In strengthening by the addition of small particles there are two cases to be considered: either the particle can be deformed with the matrix, which requires that the particle can be traversed by the dislocation, or the particle cannot be traversed by the dislocation. If the particle cannot be cut, the stress

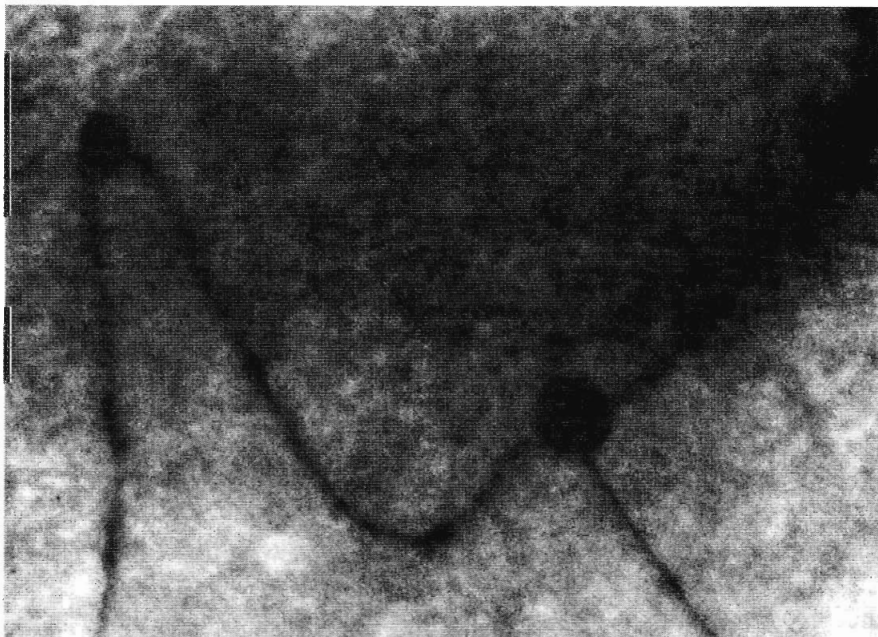


**Figure 19** Dislocations pinned by particles in magnesium oxide. (Electron micrograph by G. Thomas and J. Washburn.)

necessary to force a dislocation between particles spaced  $L$  apart on a slip plane should be approximately

$$\sigma/G = b/L . \quad (10)$$

The smaller the spacing  $L$ , the higher is the yield stress  $\sigma$ . Before particles precipitate,  $L$  is large and the strength is low. Immediately after precipitation is complete and many small particles are present,  $L$  is a minimum and the strength is a maximum. If the alloy is then held at a high temperature, some particles grow at the expense of others, so that  $L$  increases and the strength drops. Hard intermetallic phases, such as refractory oxides, cannot be cut by dislocations.

The strength of dilute solid solutions is believed to result from the pinning of dislocations by solute atoms. The solubility of a foreign atom will be greater in the neighborhood of a dislocation than elsewhere in a crystal. An atom that tends to expand the crystal will dissolve preferentially in the expanded region near an edge dislocation. A small atom will tend to dissolve preferentially in the contracted region near the dislocation—a dislocation offers both expanded and contracted regions.

As a result of the affinity of solute atoms for dislocations, each dislocation will collect a cloud of associated solute atoms during cooling, at a time when the mobility of solute atoms is high. At still lower temperatures, diffusion of solute atoms effectively ceases, and the solute atom cloud becomes fixed in the crystal. When a dislocation moves, leaving its solute cloud behind, the energy of the crystal must increase. The increase in energy can only be provided by an increased stress acting on the dislocation as it pulls away from the solute atom cloud, and so the presence of the cloud strengthens the crystal.

The passage of a dislocation across a slip plane in pure crystals does not alter the binding energy across the plane after the dislocation is gone. The internal energy of the crystal remains unaffected. The same is true for random solid solutions, because the solution is equally random across a slip plane after slip. Most solid solutions, however, have short-range order. Atoms of different species are not arranged at random on the lattice sites, but tend to have an excess or a deficiency of pairs of unlike atoms. Thus in ordered alloys dislocations tend to move in pairs: the second dislocation reorders the local disorder left by the first dislocation.

The strength of a crystalline material increases with plastic deformation. The phenomenon is called **work-hardening** or **strain-hardening**. The strength is believed to increase because of the increased density of dislocations and the greater difficulty of moving a given dislocation across a slip plane that is threaded by many dislocations. Strain-hardening frequently is employed in the strengthening of materials, but its usefulness is limited to low enough temperatures so that annealing does not occur.

An important factor in strain-hardening is the total density of dislocations. In most metals dislocations tend to form cells (Fig. 15) of dislocation-free

areas of dimensions of the order of  $1\ \mu\text{m}$ . But unless we can get a uniform high density of dislocations we cannot strain-harden a metal to its theoretical strength, because of slip in the dislocation-free areas. A high total density is accomplished by explosive deformation or by special thermal-mechanical treatments, as of martensite in steel.

Each of the mechanisms of strengthening crystals can raise the yield strength to the range of  $10^{-3}\ G$  to  $10^{-2}\ G$ . All mechanisms begin to break down at temperatures where diffusion can occur at an appreciable rate. When diffusion is rapid, precipitated particles dissolve; solute clouds drift along with dislocations as they glide; short-range order repairs itself behind slowly moving dislocations; and dislocation climb and annealing tend to decrease the dislocation density. The resulting time-dependent deformation is called creep. This irreversible motion precedes the elastic limit. The search for alloys for use at very high temperatures is a search for reduced diffusion rates, so that the four strengthening mechanisms will survive to high temperatures. But the central problem of strong alloys is not strength, but ductility, for failure is often by fracture.

### DISLOCATIONS AND CRYSTAL GROWTH

In some cases the presence of dislocations may be the controlling factor in crystal growth. When crystals are grown in conditions of low supersaturation, of the order of 1 percent, it has been observed that the growth rate is enormously faster than that calculated for an ideal crystal. The actual growth rate is explained in terms of the effect of dislocations on growth.

The theory of growth of ideal crystals predicts that in crystal growth from vapor, a supersaturation (pressure/equilibrium vapor pressure) of the order of 10 is required to nucleate new crystals, of the order of 5 to form liquid drops, and of 1.5 to form a two-dimensional monolayer of molecules on the face of a perfect crystal. Volmer and Schultze observed growth of iodine crystals at vapor supersaturations down to less than 1 percent, where the growth rate should have been down by the factor  $\exp(-3000)$  from the rate defined as the minimum observable growth.

The large disagreement expresses the difficulty of nucleating a new monolayer on a completed surface of an ideal crystal. But if a screw dislocation is present (Fig. 20), it is never necessary to nucleate a new layer: the crystal will grow in spiral fashion at the *edge* of the discontinuity shown. An atom can be bound to a step more strongly than to a plane. The calculated growth rates for this mechanism are in good agreement with observation. We expect that nearly all crystals in nature grown at low supersaturation will contain dislocations, as otherwise they could not have grown. Spiral growth patterns have been observed on a large number of crystals. A beautiful example of the growth pattern from a single screw dislocation is given in Fig. 21.

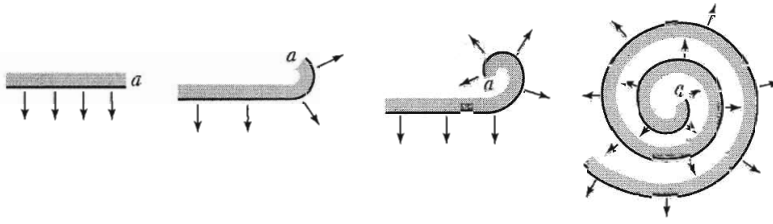


**Figure 20** Development of a spiral step produced by intersection of a screw dislocation with the surface of a crystal as in Fig. 8. (F. C. Frank.)

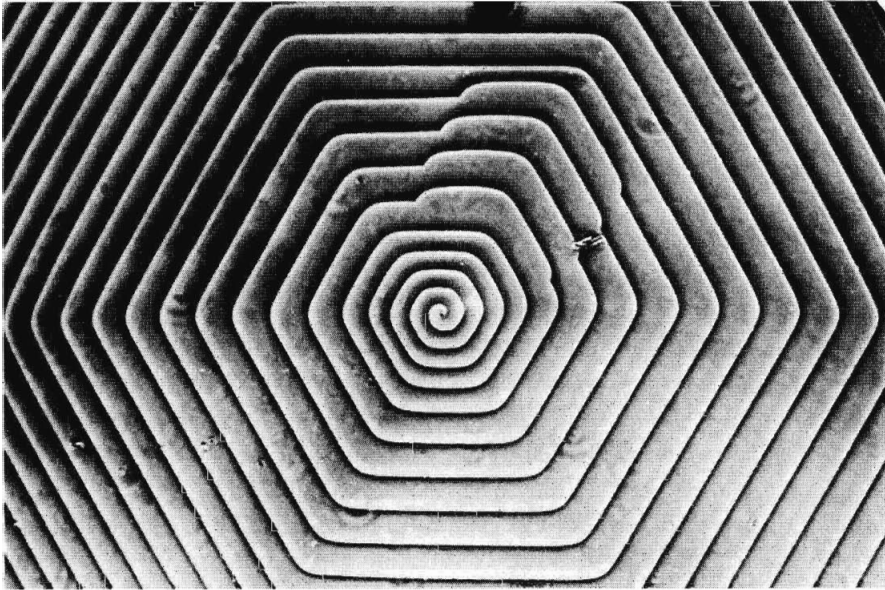


**Figure 21** Phase contrast micrograph of a hexagonal spiral growth pattern on a SiC crystal. The step height is 165 Å. (A. R. Verma.)

If the growth rate is independent of direction of the edge in the plane of the surface, the growth pattern is an Archimedes spiral,  $r = a\theta$ , where  $a$  is a constant. The limiting minimum radius of curvature near the dislocation is determined by the supersaturation. If the radius of curvature is too small, atoms on the curved edge evaporate until the equilibrium curvature is attained. Away from the origin each part of the step acquires new atoms at a constant rate, so that  $dr/dt = \text{const.}$

### **Whiskers**

Fine hairlike crystals, or **whiskers**, have been observed to grow under conditions of high supersaturation without the necessity for more than perhaps one dislocation. It may be that these crystals contain a single axial screw dislocation

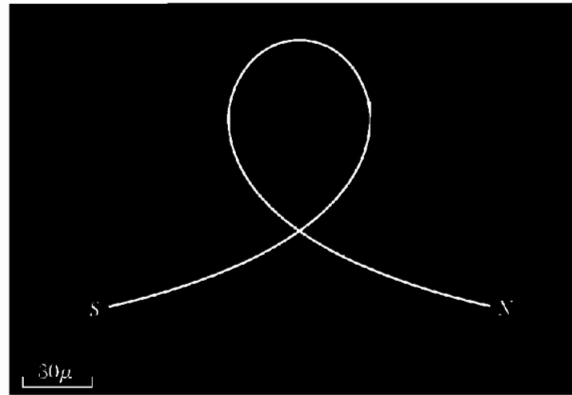


**Figure 22** A nickel whisker of diameter 1000 Å bent in a loop. (R. W. De Blois.)

that aids their essentially one-dimensional growth. From the absence of dislocations we would expect these crystal whiskers to have high yield strengths, of the order of the calculated value  $G/30$  discussed earlier in this chapter. A single axial screw dislocation, if present, could not cause yielding, because in bending the crystal the dislocation is not subjected to a shear stress parallel to its Burgers vector. That is, the stress is not in a direction that can cause slip. Herring and Galt observed whiskers of tin of radius  $\sim 10^{-4}$  cm with elastic properties near those expected from theoretically perfect crystals. They observed yield strains of the order of  $10^{-2}$ , which correspond to shear stresses of order  $10^{-2} G$ , about 1000 times greater than in bulk tin, confirming the early estimates of the strength of perfect crystals. Theoretical or ideal elastic properties have been observed for a number of materials as for carbon nanotubes. A single domain whisker of nickel is shown in Fig. 22.

### HARDNESS OF MATERIALS

The hardness of materials is measured in several ways, the simplest test for nonmetals being the scratch test. Substance A is harder than substance B if A will scratch B but B will not scratch A. A standard scale is used for representative minerals, with diamond, the hardest, assigned the value 10 and talc, the softest, assigned the value 1:

10 diamond C	5 apatite $\text{Ca}_5(\text{PO}_4)_3\text{F}$
9 corundum $\text{Al}_2\text{O}_3$	4 fluorite $\text{CaF}_2$
8 topaz $\text{Al}_2\text{SiO}_4\text{F}_2$	3 calcite $\text{CaCO}_3$
7 quartz $\text{SiO}_2$	2 gypsum $\text{CaSO}_4 \cdot 2\text{H}_2\text{O}$
6 orthoclase $\text{KAlSi}_3\text{O}_8$	1 talc $3\text{MgO} \cdot 4\text{SiO}_2 \cdot \text{H}_2\text{O}$

There is great current interest in the development of materials of great hardness, for example as films for use as scratch-resistant coatings on lenses.

It is widely felt that the scale between diamond and corundum is misleading, because diamond is much, much harder than corundum. It has been suggested that one might assign diamond the hardness 15, with the gap between 9 and 15 to be filled in eventually by synthetic materials, such as compounds of C and B.

Modern scales of hardness, such as the VHN scale, are based on indenter tests in which an indenter is pressed into the surface of the material and the size of the impression is measured. The Vickers Hardness Numbers of selected materials are tabulated below, after conversion by E. R. Weber to units of GPa [ $\text{GN/m}^2$ ]:

Diamond	45.3	BeO	7.01
SiC	20.0	Steel (quenched)	4.59
Si <sub>3</sub> N <sub>4</sub>	18.5	Cu (annealed)	0.25
Al <sub>2</sub> O <sub>3</sub>	14.0	Al (annealed)	0.12
B	13.5	Pb	0.032
WC	11.3		

The data are from J. C. Anderson and others.

### ***Problems***

- 1. Lines of closest packing.** Show that the lines of closest atomic packing are  $\langle 110 \rangle$  in fcc structures and  $\langle 111 \rangle$  in bcc structures.
- 2. Dislocation pairs.** (a) Find a pair of dislocations equivalent to a row of lattice vacancies; (b) find a pair of dislocations equivalent to a row of interstitial atoms.
- 3. Force on dislocation.** Consider a crystal in the form of a cube of side  $L$  containing an edge dislocation of Burgers vector  $\mathbf{b}$ . If the crystal is subjected to a shear stress  $\sigma$  on the upper and lower faces in the direction of slip, show, by considering energy balance, that the force acting on the dislocation is  $F = b\sigma$  per unit length.